NASA TECHNICAL NOTE

NASA TN D-4036

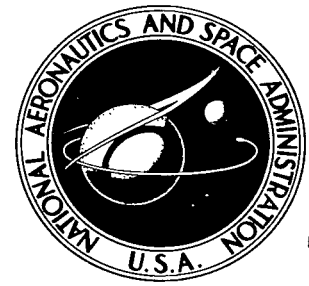

HYPERSONIC VISCOUS DRAG ON CONES IN RAREFIED FLOW

by Marvin I. Kussoy

Ames Research Center
Moffett Field, Calif.

NATIONAL AERONAUTICS AND SPACE ADMINISTRATION • WASHINGTON, D. C. • JUNE 1967

NASA TN D-4036

HYPERSONIC VISCOUS DRAG ON CONES IN RAREFIED FLOW

By Marvin I. Kussoy

Ames Research Center
Moffett Field, Calif.

NATIONAL AERONAUTICS AND SPACE ADMINISTRATION

For sale by the Clearinghouse for Federal Scientific and Technical Information
Springfield, Virginia 22151 – CFSTI price $3.00

HYPERSONIC VISCOUS DRAG ON CONES IN RAREFIED FLOW

By Marvin I. Kussoy

Ames Research Center

SUMMARY

Drag was measured in the rarefied flow regime for cones of 1° to 30° semivertex angle to determine the effects of viscous flow. The tests were conducted in the Ames 1-foot shock tunnel in air at Mach numbers of 10 and 14 and Reynolds numbers, based on cone length, of from 600 to 32,000. A free-flight experimental technique was used which avoided possible model-support sting interference effects. Drag coefficients predicted by weak-interaction theory were larger than those measured, indicating the possible presence of a merged layer which cancels a portion of the interaction effects. The viscous parameter correlated the drag data taken at both Mach numbers for the 1°, 10°, 15°, and 30° cones. For cone angles of 2.5°, 5°, and 7.5°, the $M = 10$ drag data fell below that observed for $M = 14$, indicating that any merged layer effects on these particular bodies are possibly a function of Mach number as well as the viscous parameter. Published drag measurements for wide ranges of Mach numbers (2 to 21), viscous parameters (0.02 to 0.35), cone semivertex angles (5° to 15°), and wall temperature ratios (0.02 to 1.0) were correlated by plotting the ratio of viscous drag to viscous parameter against the wall temperature ratio.

INTRODUCTION

Viscous flow over cones has been the subject of several recent experimental and theoretical studies. Slender cone surface pressures at supersonic Mach numbers can be predicted (ref. 1) by weak-interaction theory, which assumes a Rankine-Hugoniot shock, and separate viscous and inviscid flow regions over the body. At hypersonic Mach numbers and low Reynolds numbers, however, neither cone surface pressure nor heat-transfer results show any interaction effects (refs. 2-5). In addition, the experimental flow field studies (ref. 5) have found a weakened shock structure and a fully merged viscous region at the same test conditions. Consequently, there has been some question as to what parameter to use (i.e., what flow mechanism is dominating) to correlate data such as surface pressures, heat transfer, and drag coefficients.

The present investigation was made to determine the effect of viscous flow on the drag of cones. Purposes of this study included extending available experimental data to a wider range of cone angles and attempting to correlate these data with data obtained in other experimental investigations.

SYMBOLS

C_D drag coefficient, referenced to model base area

C_∞ Chapman-Rubesin viscosity coefficient

M Mach number

Re Reynolds number

T temperature

$\bar{v}_\infty$ viscous parameter, $\frac{M_\infty \sqrt{C_\infty}}{\sqrt{Re_{\infty,l}}}$

θ_c cone semivertex angle

Subscripts

FM free molecule value

inv inviscid value

l length

w wall

∞ free-stream conditions

o stagnation conditions

EXPERIMENTAL PROCEDURE

Facility and Test Conditions

The tests were performed in the Ames 1-foot combustion driven shock tunnel, described in references 6 and 7. This facility is operated in air at nominal free-stream Mach numbers of 10 and 14 and nominal Reynolds numbers per inch of 5,000 and 8,000, respectively. The nominal reservoir pressure and temperature for the tests were approximately 4,200 psia and 10,500° R for both Mach numbers. The useful testing time of this facility is approximately 25 milliseconds.

Models

The semivertex angle of the cone models tested ranged from 1° to 30°. In order to obtain a Reynolds number variation, the models were made of various lengths. To insure a reasonable static stability margin, the model nose was made of mild steel and the base of either plastic or wood. These two materials were first glued together and then machined. A set of 5° cones, varying in length from 0.38 to 4 inches, is shown in figure 1. For the present test conditions, the mean free path in the free stream was approximately 0.003 inch. Photomicrographs indicated that the model tips were approximately 0.0005 inch in diameter. Thus the cones were considered sharp for the aerodynamic purposes of the present study.

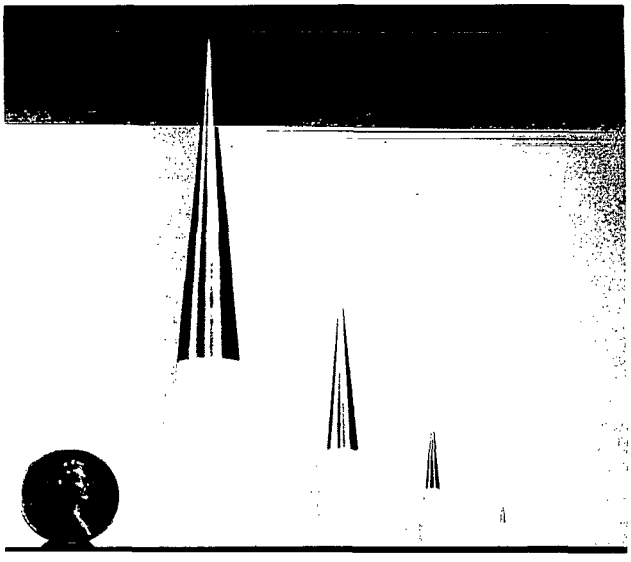

Figure 1.- Typical models investigated.

Test Procedure and Instrumentation

To insure data free of sting interference, a free-flight technique was used for measuring the cone drag coefficient. This method is similar to that used in a shock tunnel at the Naval Ordnance Laboratory (see refs. 8 and 9). The models and "calibrating spheres" (spheres having known drag coefficients) are suspended from a frame in the test section by means of thin nylon filaments, 0.5 mil in diameter. The initial flow burns away these threads in approximately 1 msec, leaving the models suspended in the test section at, or near, zero angle of attack. Some cone models went to a high angle of attack either because the strings burned unevenly or because of tunnel transients. The data from these models were discarded. Only data from cone models at angles of attack below $\pm 2^{\circ}$ were used in this study. Figure 2 is a sketch of a typical test setup. Two high-speed 16-mm cameras operating at 2000 frames/second recorded the flight of the cones and reference spheres as viewed through the side and top windows.

Data Reduction and Precision

Model movement as a function of time was obtained from the filmed flight. When the model acceleration is constant, the distance traveled will vary with the time squared. Therefore, the model distance was plotted against time squared and a straight line was fitted to the data to determine the acceleration of the model.

Since the dynamic pressure of the tunnel varied about ±20 percent from run to run, a convenient method for obtaining the drag coefficient of the

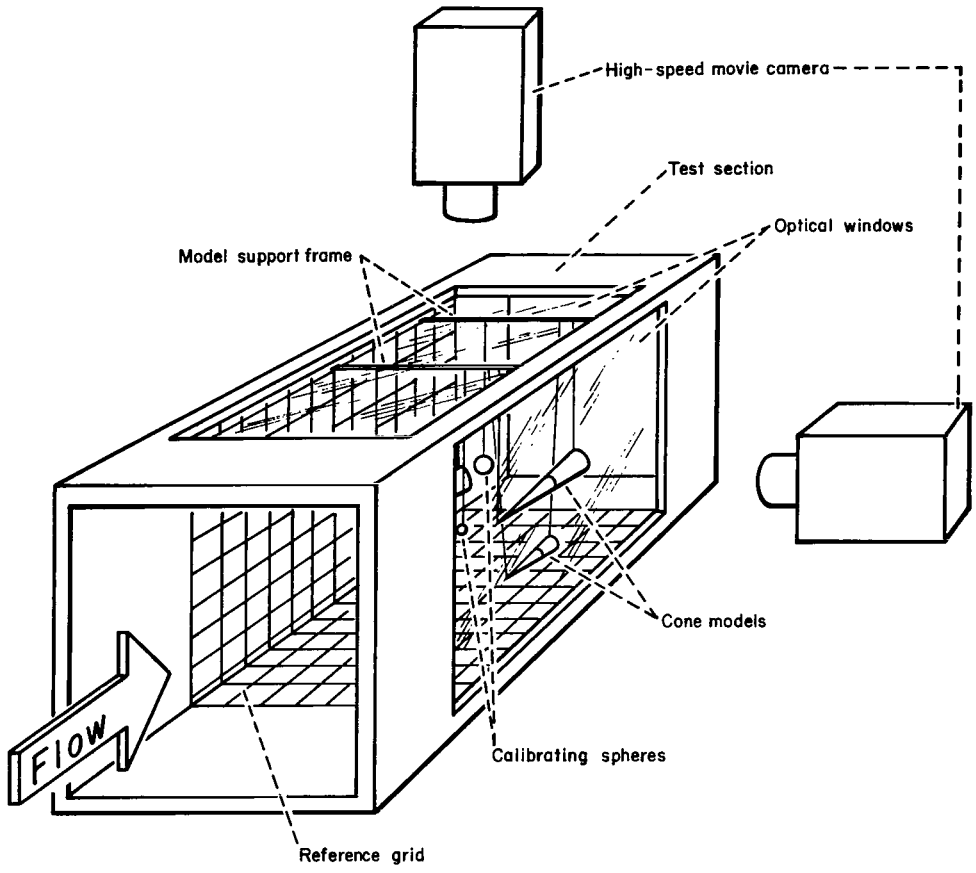

Figure 2.- Typical test-run setup.

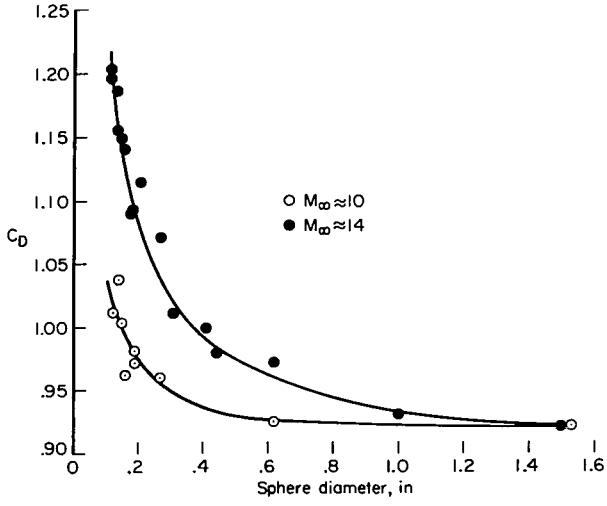

Figure 3.- Drag coefficients of calibrating spheres.

cones was to include a small sphere of known drag coefficient in each run (thus reducing the uncertainty in knowing the stream dynamic pressure), and compute the cone drag coefficient from the sphere drag coefficient and the sphere and cone mass and acceleration ratios. The drag coefficient of the small sphere was obtained by measuring simultaneously the drag of various sizes of spheres and comparing it with the drag of a large sphere (1.5 in. diam) that was definitely in the continuum flow regime; the results are given in figure 3. The large sphere was assigned a drag coefficient of 0.92, as determined in reference 10 for continuum flow. This large sphere was also run with a pitot probe in the

test stream. Since the ratio of dynamic pressure to pitot pressure is essentially constant for hypersonic Mach numbers, the drag coefficient can be obtained from this ratio and the acceleration of the sphere. A drag coefficient of 0.92 ±0.05 was obtained for the large sphere in this manner. For the present investigation of cone drag, the drag coefficients of the calibrating spheres (0.15 to 0.35 in. diam) were obtained from the fairing of the data of figure 3.

The method described above introduced errors in sphere drag coefficient estimated to be less than ±5 percent. Thus it is believed that an experimental accuracy of ±5 percent for the sphere calibration data and ±10 percent for the cone drag data (since the cone data depends directly on the sphere drag) is the best obtainable for the present series of tests.

RESULTS AND DISCUSSION

Present Test Results

The data from the present tests are compared in figure 4 with theoretical drag coefficients. Both data and theory are plotted against the viscous parameter, $\bar{v}_\infty$ ($\equiv M_\infty \sqrt{C_\infty} / \sqrt{Re_{\infty,\zeta}}$), for nominal test Mach numbers of 10 and 14. For reference purposes, the calculated inviscid and free molecular drag coefficients are also shown. The inviscid value was computed from the tunnel nominal running conditions, assuming the base pressure equaled the free-stream static pressure. The drag coefficient for free molecular flow was computed for the present test conditions for diffuse reflection by the method given in reference 11 (assuming an accommodation coefficient of unity). For simplicity, only two viscous flow calculations are shown - one composed of five separate terms, and the other of only two terms. The former computation, similar to that of reference 12, used the following five terms:

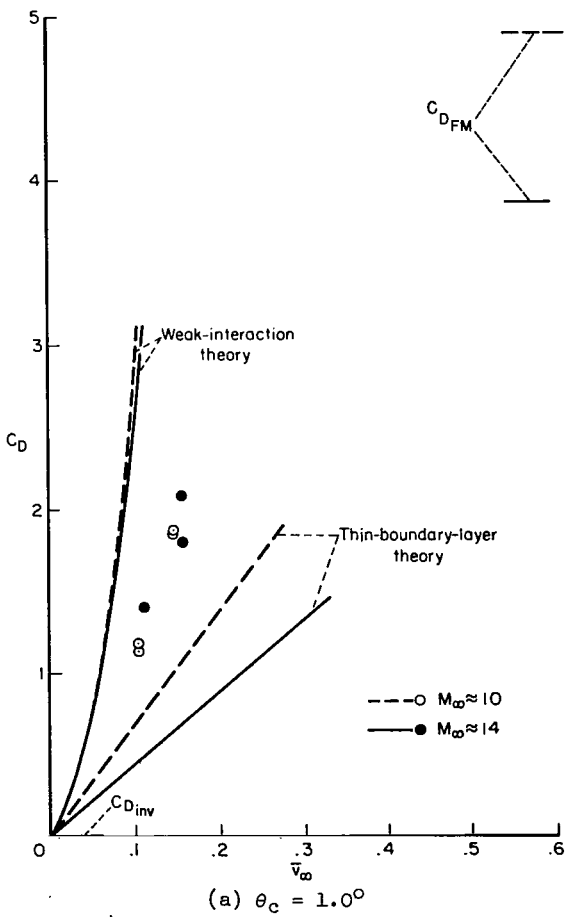

(a) $\theta_c = 1.0^\circ$

Figure 4.- Viscous drag data on sharp cones.

1. Inviscid pressure drag.

2. Skin-friction drag for zero pressure gradient. The exact solutions of Van Driest (ref. 13), modified by the Mangler transformation, were used to compute this term.

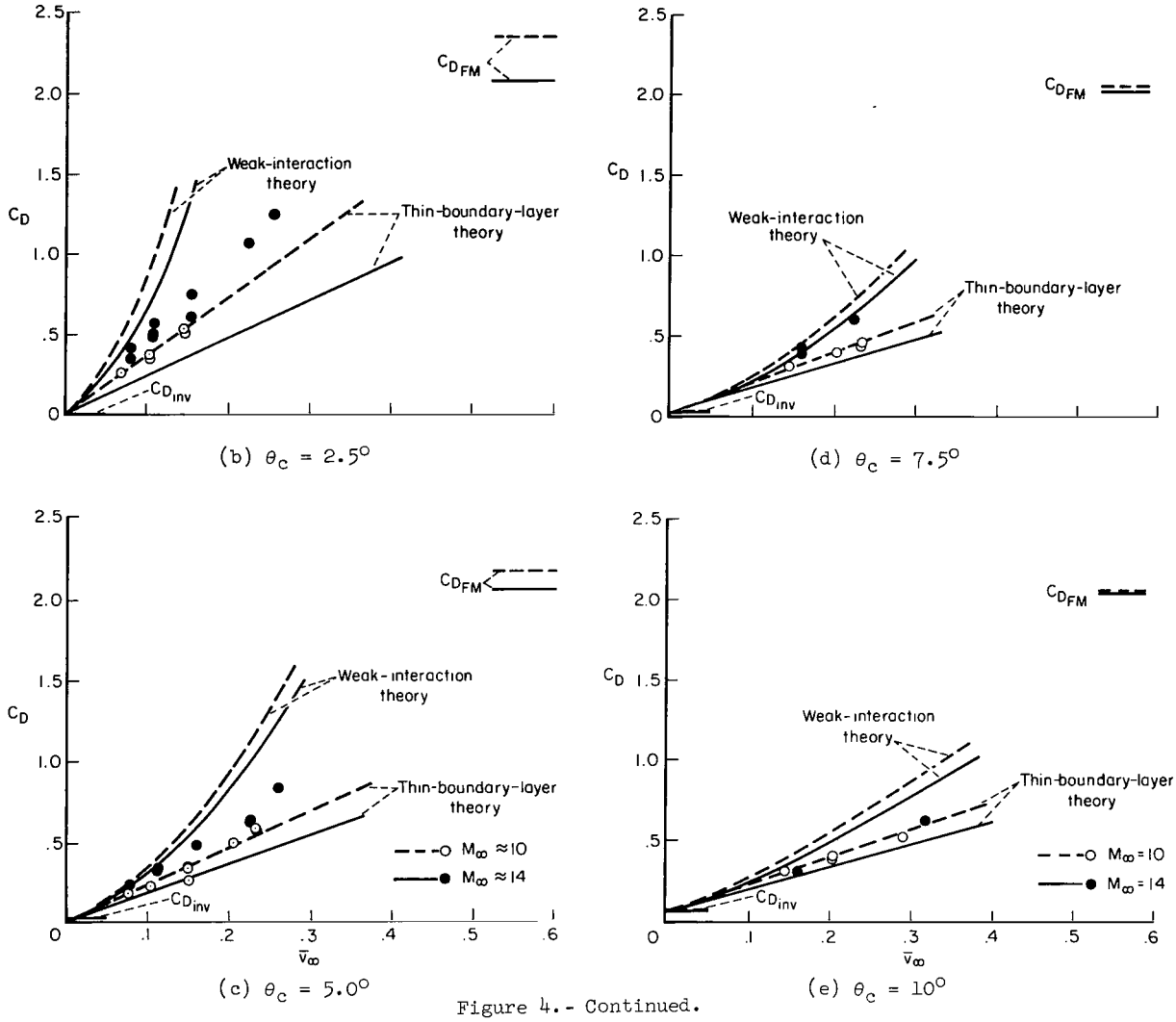

Figure 4.- Continued.

3. Induced pressure drag derived from the change in effective aerodynamic body shape due to the boundary layer as formulated by Probstein (ref. 14).

4. Incremental increase in the zero pressure gradient skin-friction drag due to the presence of an induced pressure gradient. This term was developed by Probstein (ref. 14).

5. Transverse curvature skin-friction drag; the increment to the zero pressure gradient skin friction due to the relatively large boundary-layer thickness in relation to the body radius. This term is given by Probstein and Elliott (ref. 15).

The linear combination of the above five terms will be called the weak-interaction theory. The two-term theory, consisting of only the first two terms discussed above, will be called the thin-boundary-layer theory. For the wide range of cone angles considered, the measured drag coefficients vary

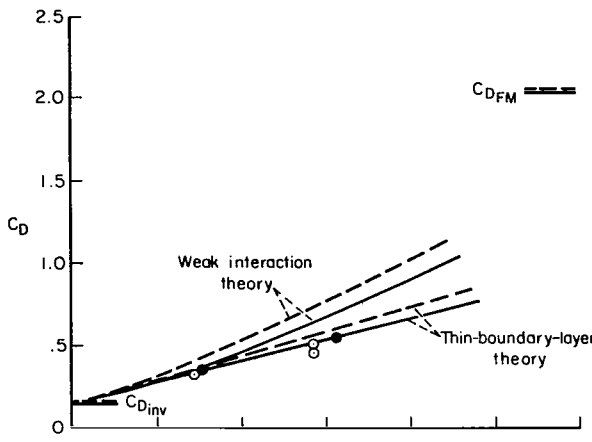

(f) $\theta_c = 15^\circ$

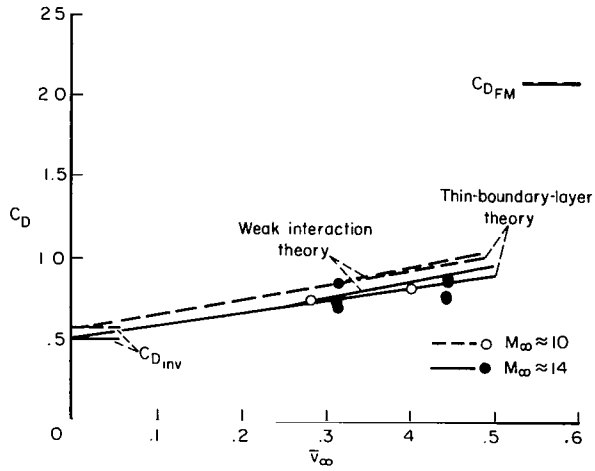

(g) $\theta_c = 30^\circ$

Figure 4.- Concluded.

linearly (within experimental accuracy) with $\bar{v}_\infty$. This result agrees with the observations of references 16 and 17. The drag predicted by weak-interaction theory is generally too large, particularly at the smaller cone angles. (The apparent agreement of the data taken with the 7.5° cone at Mach 14 with the weak-interaction theory will be discussed below.) The measured drag coefficients were less than about half of the free molecule value at the highest $\bar{v}_\infty$ tested.

For $\bar{v}_\infty \approx 0.2$, weak-interaction effects on slender cones have been found at a lower Mach number ($M \approx 4$, ref. 1) whereas no interaction effects, in fact, a merged layer, have been found at a higher Mach number ($M = 24$, ref. 5). The present tests span a range of Mach numbers, viscous parameters, and cone angles of considerable interest. At the larger cone angles tested ($10^\circ < \theta_c < 30^\circ$) and at the smallest cone angle (1°) there appears to be no Mach number effect, and the data are correlated within experimental accuracy by the viscous parameter, $\bar{v}_\infty$. At the intermediate cone angles, from 7.5° to 2.5°, inclusive, the $M = 14$ drag data are higher than those obtained at $M = 10$; the viscous parameter ($\bar{v}_\infty$) does not correlate these data. The general disagreement of the data with weak-interaction theory may be due to a "cancelling effect" caused by the presence of a merged layer. The failure of the viscous parameter to correlate the intermediate cone-angle data indicates that the extent of a merged flow field on a slender body depends on some other function of Reynolds number and Mach number than that contained in the viscous parameter. In light of the above discussion, it is felt that the agreement of the $M = 10$ data with the thin-boundary-layer theory for $7.5^\circ > \theta > 2.5^\circ$, and the $M = 14$ data at $\theta_c = 7.5^\circ$ with the weak-interaction theory is fortuitous. Evidently theoretical work is needed to develop a valid flow model for slender axisymmetric bodies that will be consistent with the experimental observations of references 2 to 5 and those of the present work.

Comparison With Other Results

There have been several investigations of viscous drag on sharp and slightly blunted cones published recently. Data have been obtained over a wide range of Mach numbers, wall temperature ratios, and viscous parameters on cones with semivertex angles of from 5° to 15°. Tests have included free-flight and sting-mounted models in continuously running low-density tunnels, ballistic ranges, and shock tunnels. These data, divided into groups of approximate cone angles of 5°, 10°, and 15°, are plotted in the form C_D vs. $\bar{v}_\infty$ in figure 5. Data are also shown for slightly blunted cones. It has been found experimentally (refs. 12 and 17) that ratios of nose radius to base radius (R_N/R_B) of up to 0.1 have small effects on measured drag coefficients. The pertinent data from the present series of tests are also shown for comparison. The viscous parameter does not collapse these data when plotted in this manner. However, since drag coefficient varies linearly with the viscous parameter for a given set of free-stream conditions, wall temperature ratios, and cone angles, an attempt is made to correlate the available data by plotting the quantity $(C_D - C_{D_{inv}})/\bar{v}_\infty$ against the wall temperature ratio, T_w/T_o (fig. 6). It was hoped that the viscous parameter might account for any variations in Mach number and Reynolds number, and that wall temperature ratio would correlate any additional changes in the boundary-layer flow over the body. However, the Mach number effect previously discussed is still present in this correlation. All available data (refs. 12, 16-21) have been presented in this manner in figure 6, and fall within the lightly shaded

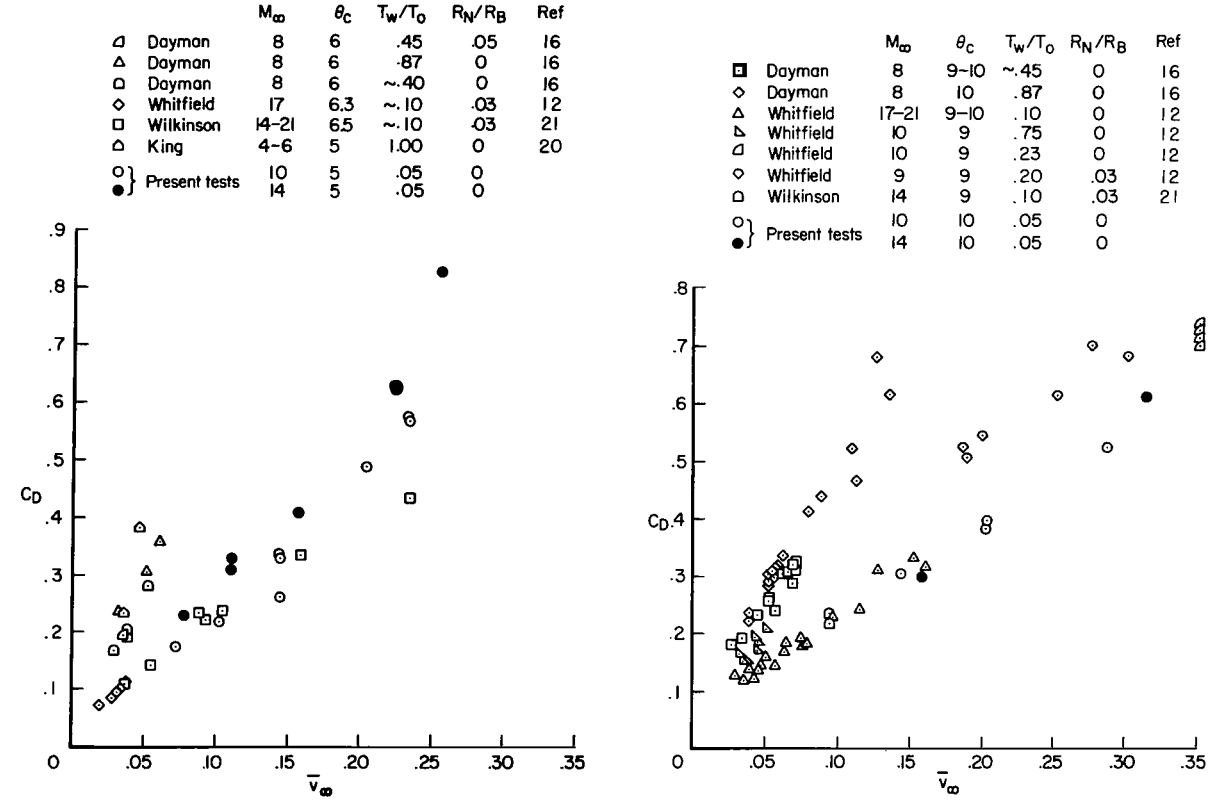

(a) $\theta_c \approx 5^\circ$ (b) $\theta_c \approx 10^\circ$

Figure 5.- Comparison of published data with present results.

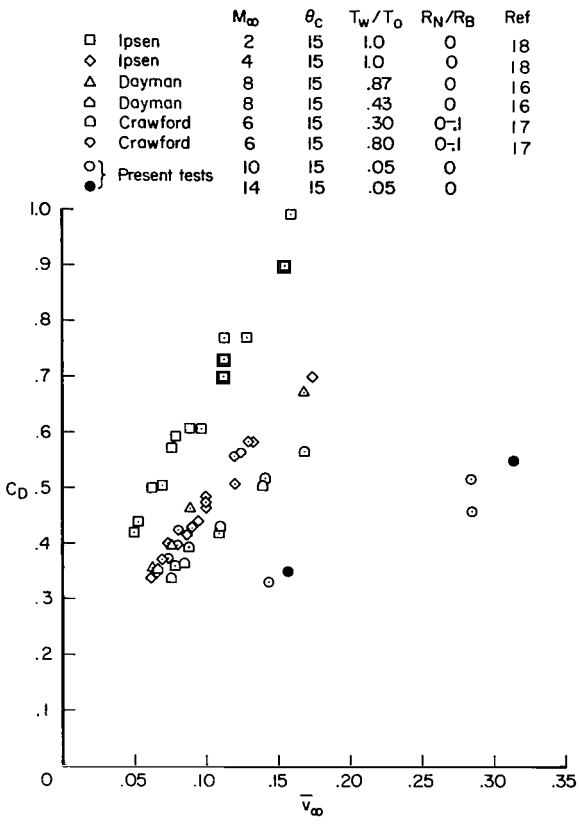

(c) $\theta_c \approx 15^\circ$

Figure 5.- Concluded.

region. (Data are available at only several discrete values of T_w/T_o, as indicated in fig. 5. For simplicity, a continuous band is shown in fig. 6 instead of the individual data points.) The range of data from the present tests for angles of 5° to 15° is also indicated. The drag computed by weak-interaction theory for all the test conditions is shown as solid vertical lines. Also indicated on this figure are the maximum values of $\bar{v}_\infty$ encountered for each specific set of available data. It is evident from this plot that the data collapse in a relatively narrow band whereas the theoretical calculations do not. For small values of the viscous parameter, weak-interaction theory appears to predict the drag adequately. However, for large values of the viscous parameter there is a large difference between the experimental values and those predicted by weak-interaction theory. This again points up the inadequacy of this theory and indicates the need for further study to determine the relative contribution of low-density effects to the drag of slender bodies and to determine the corresponding appropriate correlating parameters.

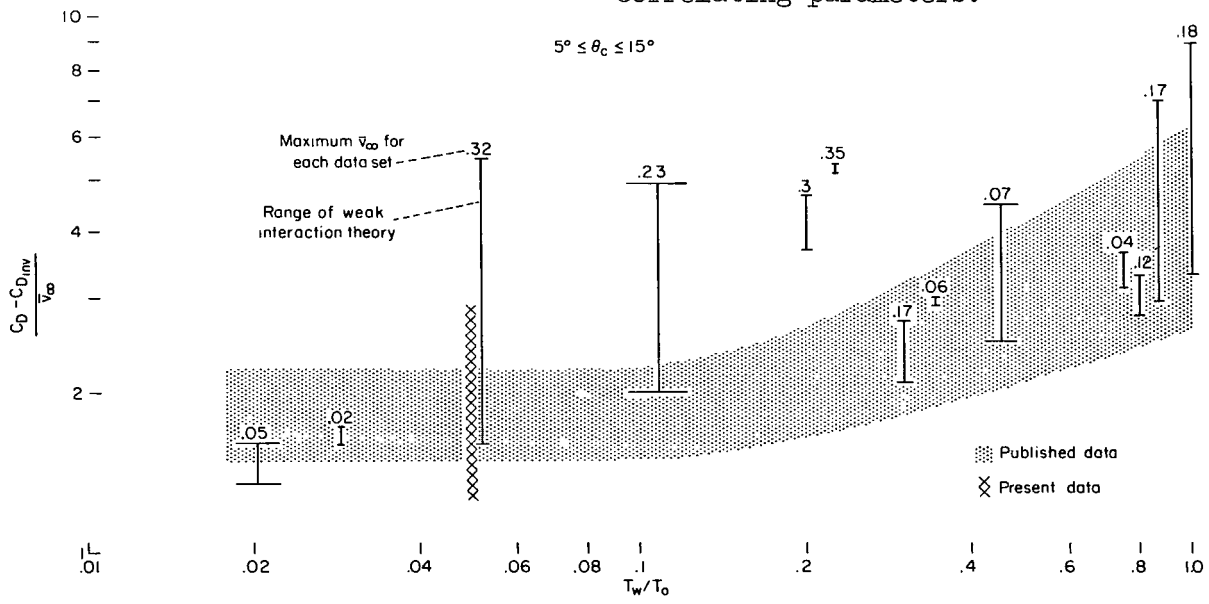

Figure 6.- Correlation of published data and comparison with theory; $5^\circ \le \theta_c \le 15^\circ$.

SUMMARY OF RESULTS

Drag coefficients were obtained for sharp cones at zero angle of attack in low-density hypersonic flow. Cone semivertex angle, θ_c, varied from 1° to 30°, and the viscous parameter $\bar{v}_\infty$ varied from 0.07 to 0.45. Specific results are as follows:

1. The drag coefficient for the cones increased linearly with increasing viscous parameter to about half the free molecule value at the highest $\bar{v}_\infty$ tested.

2. Drag coefficients predicted by weak-interaction theory were higher than the experimental results for all cone angles, indicating the possible presence of a merged layer that cancels a portion of the interaction effects.

3. The viscous parameter correlated the drag data taken at Mach numbers of 10 and 14 for the 1°, 10°, 15°, and 30° cones. For cone angles of 2.5°, 5°, and 7.5°, the $M = 10$ drag data fell below that observed for $M = 14$, indicating that any effects of a merged layer on these particular bodies are possibly some other function of Mach number and Reynolds number than that contained in the viscous parameter.

4. Published cone drag data obtained over a broad range of test conditions were correlated by plotting the quantity $(C_D - C_{D_{inv}})/\bar{v}_\infty$ against wall temperature ratio. Predictions by weak-interaction theory were also made. For small values of the viscous parameter, the weak-interaction theory adequately predicted the drag data. The inadequacy of this theory at high values of the viscous parameter indicates the need for further research to determine the relative contribution of rarefied effects to the drag of slender cones.

Ames Research Center
National Aeronautics and Space Administration
Moffett Field, California, 94035, March 30, 1967
124-07-02-14-00-21

REFERENCES

1. Talbot, L.; Koga, T.; and Sherman, P. M.: Hypersonic Viscous Flow Over Slender Cones. J. Aerospace Sci., vol. 26, no. 11, Nov. 1959, pp. 723-730.

2. Burke, A. F.; and Dowling, E. D.: Aerodynamic Aspects of the Use of a Blunt, Slender Cone as an Air-Data Probe at Hypersonic Speeds. Rep. AA-1577-Y-4, Cornell Aero. Lab., Nov. 1962.

3. Lewis, Clark H.; Marchand, Ernest O.; and Little, Herbert R.: Mass Transfer and First-Order Boundary-Layer Effects on Sharp Cone Drag. AIAA Paper 66-33, 1966.

4. Waldron, H. F.: Viscous Hypersonic Flow Over Pointed Cones at Low Reynolds Numbers. AIAA Paper 66-34, 1966.

5. McCroskey, W. J.; Bogdonoff, S. M.; and Genchi, A. P.: Leading Edge Flow Studies of Sharp Bodies in Rarefied Hypersonic Flow. Presented at Fifth Rarefied Gas Dynamics Symposium, Oxford, England, July 1966.

6. Cunningham, Bernard E.; and Kraus, Samuel: A 1-Foot Hypervelocity Shock Tunnel in Which High-Enthalpy, Real Gas Air Flows can be Generated With Flow Times of About 180 Milliseconds. NASA TN D-1428, 1962.

7. Loubsky, William J.; Hiers, Robert S.; and Stewart David A.: Performance of a Combustion Driven Shock Tunnel With Application to the Tailored-Interface Operating Conditions. Presented at 3rd Conf. on Performance of High Temperature Systems, Pasadena, Calif., Dec. 1964.

8. Aronson, P. M.; Marshall, T.; Seigel, A. E.; Slawsky, Z. I.; and Smiley, E. F.: Shock Tube Wind Tunnel Research at the U. S. Naval Ordnance Laboratory. Proc. Second Shock-Tube Symp., Palo Alto, Calif., March 5-6, 1958. Air Force Special Weapons Center, SWR-TM-58-3, pp. 4-27.

9. Gates, D. F.; and Bixler, D. N.: The Measurement of Aerodynamic Forces and Moments in the NOL 4 Inch Hypersonic Shock Tunnel No. 3. NOLTR 61-100, Sept. 7, 1961.

10. Hodges, A. J.: The Drag Coefficient of Very High Velocity Spheres. J. Aerospace Sci., vol. 24, no. 10, Oct. 1957, pp. 755-758.

11. Stalder, Jackson R.; and Zurick, Vernon J.: Theoretical Aerodynamic Characteristics of Bodies in a Free-Molecule-Flow Field. NACA TN 2423, 1951.

12. Whitfield, Jack D.; and Griffith, B. J.: Hypersonic Viscous Drag Effects on Blunt Slender Cones. AIAA J., vol. 2, no. 10, Oct. 1964, pp. 1714-1722.

13. Van Driest, E. R.: Investigation of Laminar Boundary Layer in Compressible Fluids Using the Crocco Method. NACA TN 2597, 1952.

14. Probstein, Ronald F.: Interacting Hypersonic Laminar Boundary Layer Flow Over a Cone. Tech. Rep. AF 2798/1, Brown Univ., Div. of Engr. Contract AF 33(616)-2798, March 1955.

15. Probstein, Ronald F.; and Elliott, David: The Transverse Curvature Effect in Compressible Axially Symmetric Laminar Boundary-Layer Flow. Rep. 261, Princeton Univ., Dept. of Aeronautical Engr., Apr. 1954, pp. 23, 208-236.

16. Dayman, Bain, Jr.: Hypersonic Viscous Effects on Free-Flight Slender Cones. AIAA J., vol. 3, no. 8, Aug. 1965, pp. 1391-1400.

17. Crawford, D. R.: Wall Temperature Effects on the Zero-Lift Viscous Drag of Blunted Cones in Rarefied Supersonic Flow. Rep. AS-65-15, University of California, Berkeley, Sept. 1965.

18. Ipsen, D. C.: Experiments on Cone Drag in a Rarefied Air Flow. Jet Propulsion, vol. 26, no. 12, Dec. 1956, pp. 1076-1077.

19. Lyons, W. C., Jr.; Brady, J. J.; and Levensteins, Z. J.: Hypersonic Drag, Stability, and Wake Data for Cones and Spheres. AIAA J., vol. 2, no. 11, Nov. 1964, pp. 1948-1956.

20. King, Hartley H.; and Talbot, Lawrence: Effect of Mass Injection on the Drag of a Slender Cone in Hypersonic Flow. AIAA J., vol. 2, no. 5, May 1964, pp. 836-844.

21. Wilkinson, David B.; and Harrington, Shelby A.: Hypersonic Force, Pressure, and Heat Transfer Investigations of Sharp and Blunt Slender Cones. AEDC-TDR-63-177, Cornell Aero. Lab., Buffalo, N. Y., Aug. 1963.

"The aeronautical and space activities of the United States shall be conducted so as to contribute . . . to the expansion of human knowledge of phenomena in the atmosphere and space. The Administration shall provide for the widest practicable and appropriate dissemination of information concerning its activities and the results thereof."

—NATIONAL AERONAUTICS AND SPACE ACT OF 1958

NASA SCIENTIFIC AND TECHNICAL PUBLICATIONS

TECHNICAL REPORTS: Scientific and technical information considered important, complete, and a lasting contribution to existing knowledge.

TECHNICAL NOTES: Information less broad in scope but nevertheless of importance as a contribution to existing knowledge.

TECHNICAL MEMORANDUMS: Information receiving limited distribution because of preliminary data, security classification, or other reasons.

CONTRACTOR REPORTS: Scientific and technical information generated under a NASA contract or grant and considered an important contribution to existing knowledge.

TECHNICAL TRANSLATIONS: Information published in a foreign language considered to merit NASA distribution in English.

SPECIAL PUBLICATIONS: Information derived from or of value to NASA activities. Publications include conference proceedings, monographs, data compilations, handbooks, sourcebooks, and special bibliographies.

TECHNOLOGY UTILIZATION PUBLICATIONS: Information on technology used by NASA that may be of particular interest in commercial and other non-aerospace applications. Publications include Tech Briefs, Technology Utilization Reports and Notes, and Technology Surveys.

Details on the availability of these publications may be obtained from:

SCIENTIFIC AND TECHNICAL INFORMATION DIVISION

NATIONAL AERONAUTICS AND SPACE ADMINISTRATION

Washington, D.C. 20546